A highly reduced cyanogen ligand derived from cyanide reductive coupling†‡

Alexander R. Fox and Christopher C. Cummins*

The synthesis, structure, and spectroscopic features of a bimetallic cyanogen complex obtained from the reductive coupling of cyanide by a niobium(IV) precursor are described, and a mechanism for the coupling reaction is proposed based on DFT calculations.

The study of metal-mediated reductive coupling of unsaturated substrates traces its roots to Fittig who in 1859 described the coupling of acetone to pinacol with sodium metal.[1] The scope and facility of reductive coupling chemistry has since expanded to include reductants from across the *d*- and *f*-blocks and a range of unsaturated substrates, including imines, nitriles, isocyanides, CO, CO_2, and CS_2.[2–15] Despite this wealth of chemistry, very few examples exist for the reductive coupling of cyanide to polycyanide derivatives such as cyanogen (N≡C–C≡N). Long and co-workers demonstrated reductive tetramerization of cyanide with the vanadium(III) complex $(Me_3tacn)V(OTf)_3$ (Me_3tacn = N,N',N''-trimethyl-1,4,7-triaza-cyclononane) and LiCN·DMF (DMF = dimethylformamide), yielding the structurally characterized bimetallic vanadium(IV) product $(\mu\text{-}C_4N_4)[V(CN)_2(Me_3tacn)]_2$·2.5DMF, where $\mu\text{-}C_4N_4$ is formulated as a tetraanionic *trans*-dicyanoethenediimide ligand.[16] Beyond this report, however, the metal-mediated coupling of cyanide is limited to oxidative coupling reactions.[17,18]

In the course of exploring the metal–ligand multiple bonding chemistry of a niobium tris(anilide) platform,[19] we encountered a unique example of cyanide coupling. Stirring a purple-brown solution of the niobium(IV) triflate complex $(TfO)Nb(N[Np]Ar)_3$ (**1**; Np = CH_2-t-Bu; Ar = $3,5\text{-}Me_2C_6H_3$) and solid NaCN in THF resulted in a gradual color change to orange-brown over *ca.* 18 h. An orange powder was obtained in 91% yield following separation from NaOTf and precipitation from Et_2O (Scheme 1).

The ^{1}H NMR spectrum of the isolated material revealed no paramagnetically broadened or shifted features, but rather

displayed a set of resonances for a single *N*-neopentylanilide ligand environment in a diamagnetic complex. Acknowledging the highly reducing nature of low-valent early transition metal complexes and their ability to effect the reductive coupling of unsaturated ligands,[3,9,20–23] we hypothesized that the reaction under investigation led to the initial formation of the d^1 C-bound cyanide complex $(NC)Nb(N[Np]Ar)_3$, which then coupled to form the bimetallic μ-cyanogen complex $(\mu,\eta^1:\eta^1\text{-}NCCN)[Nb(N[Np]Ar)_3]_2$ (**2**). The reductive coupling of two cyanide ions was confirmed by a single-crystal X-ray diffraction study of the isolated material, and its Raman and multinuclear NMR spectroscopic features provided additional support for this formulation.

Complex **2** crystallized in the orthorhombic space group *Pbca* with one-half of the total molecule contained in the asymmetric unit. A crystallographic inversion center residing at the midpoint of the central C≡C bond generates the entire molecule and imparts **2** with rigorous C_i point symmetry (Fig. 1). Each niobium center is coordinated by three *N*-neopentylanilide ligands in a *quasi-C_3* fashion and occupies a terminus of a linear Nb≡N–C≡C–N≡Nb array.[24] The Nb1–N4 and C4–C4A distances of 1.7920(17) and 1.220(4) Å are consistent with Nb–N and C–C triple bonds, respectively.[25] The notably short N4–C4 distance of 1.306(3) Å is intermediate between a C–N single and double bond,[26] and the Nb1–N4–C4 and N4–C4–C4A angles of 177.66(17) and 178.6(3)°, respectively, illustrate the linearity of the central Nb≡N–C≡C–N≡Nb core. Structurally characterized complexes featuring cyanogen as a bridging ligand are rare and are limited to cases involving
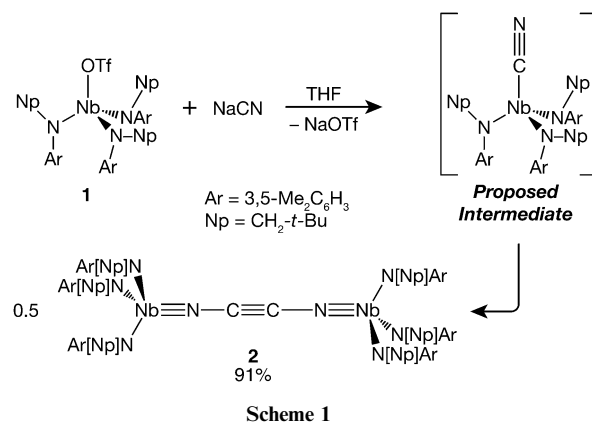
Department of Chemistry, Massachusetts Institute of Technology,
77 Massachusetts Avenue, Room 6-435, Cambridge, MA 02139-4307,
USA. E-mail: ccummins@mit.edu; Fax: +1 (617) 253-5332;
Tel: +1 (617) 253-7670
† Reproduced in part with permission from: A. R. Fox, PhD thesis, Massachusetts Institute of Technology, 2010.
‡ Electronic supplementary information (ESI) available: NMR and Raman spectroscopic data, crystallographic data, and computational details. See DOI: 10.1039/c2cc17212g


Scheme 1
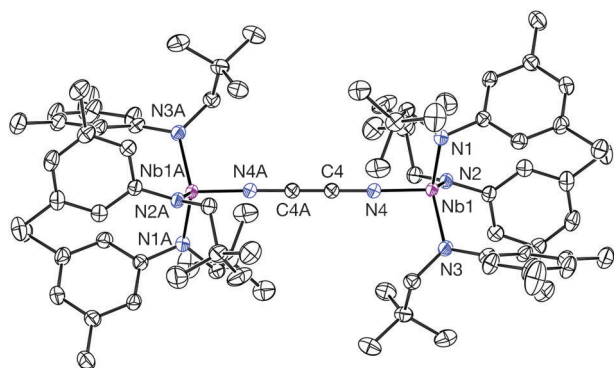
Fig. 1 Thermal ellipsoid plot[30] of **2**, drawn at 50% probability and with hydrogen atoms omitted for clarity. Selected distances (Å) and angles (°): Nb1–N4, 1.7920(17); N4–C4, 1.306(3); C4–C4A, 1.220(4); avg. Nb–N$_{anilide}$, 2.0173(10); Nb1–N4–C4, 177.66(17); N4–C4–C4A, 178.6(3).

Fig. 2 *Top*: Raman spectra of **2** and its labeled isotopologues **2**-^{13}C and **2**-^{15}N. *Bottom*: Resonances associated with the μ-^{15}NCC^{15}N ligand in the ^{13}C{^{1}H} and ^{15}N NMR spectra of **2**-^{15}N.

Lewis acid/base complexes of closed shell transition metal or main group metalloid centers.[27,28] In these cases, the internal C–N and C–C distances of the μ-cyanogen ligand are largely unchanged from those of free cyanogen (d(C–N) = 1.13(2) Å; d(C–C) = 1.37(2) Å).[29] In contrast, the structural metrics and diamagnetism of **2** point to a bridging ligand that may be formulated as a highly reduced ethynediimide (NCCN^{4-}) ion.

The isotopically labeled complexes (μ,η^1:η^1-N^{13}C^{13}CN)-[Nb(N[Np]Ar)$_3$]$_2$ (**2**-^{13}C) and (μ,η^1:η^1-^{15}NCC^{15}N)[Nb(N[Np]-Ar)$_3$]$_2$ (**2**-^{15}N) were prepared in 44% and 94% yield, respectively, by the reaction of **1** with K^{13}CN/15-crown-5 or NaC^{15}N. The low yield for **2**-^{13}C is attributed to the lower solubility of K^{13}CN as compared to NaCN or NaC^{15}N. The ^{13}C{^{1}H} NMR spectrum of **2**-^{13}C shows a strong singlet at δ = 79.49 ppm, which is within a region typical for alkynyl groups.[31] The ^{15}N NMR spectrum of **2**-^{15}N shows only one feature, a singlet at δ = 337.1 ppm (*vs*. PhC^{15}N, δ = 258.4), while the ^{13}C{^{1}H} NMR spectrum of **2**-^{15}N contains a weak doublet at 79.51 ppm that evinces nuclear spin coupling within the NCCN unit with $^1J_{CN}$ = 26.4 Hz. The Raman spectra of **2**, **2**-^{13}C, and **2**-^{15}N were recorded using solid powdered samples and laser excitation at 785 nm. In all three spectra, two intense bands were observed (Fig. 2). In **2**, these peaks are found at ν = 1132 and 2060 cm^{-1}, while in **2**-^{13}C these peaks shift to ν = 1129 and 1983 cm^{-1}, and in **2**-^{15}N they shift to ν = 1091 and 2046 cm^{-1}, indicating that the lower energy band is associated with C–N oscillation and the higher energy band is associated with C–C oscillation. The Raman bands in (**2**-^{13}C) and (**2**-^{15}N) differ in energy from that predicted by a simple two-body harmonic oscillator model (**2**-^{13}C: ν = 1085, 1902 cm^{-1}; **2**-^{15}N: ν = 975 cm^{-1}, 2060 cm^{-1}), suggesting that these modes are coupled to each other or to other oscillators within the molecule.[32]

Calculations performed on the centrosymmetric model complex (μ,η^1:η^1-NCCN)[Nb(N[Me]Ph)$_3$]$_2$ (**3**) at the density functional theory (DFT) level (TZ2P/ZORA/OLYP)[33] provided an optimized geometry for **3** that agrees well with that of **2**. The Raman active modes associated with the central μ-NCCN ligand in **3** are predicted by these calculations to occur at ν = 1019 and 2119 cm^{-1} (uncorrected).[34] The frontier
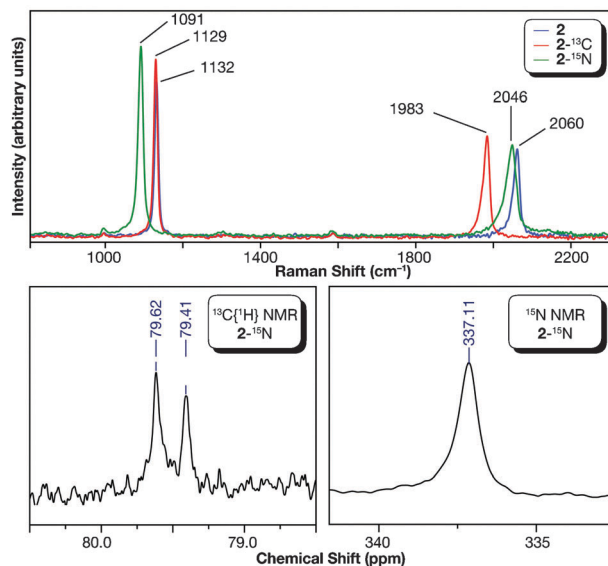
molecular orbitals in **3** emanate from the π-system of the Nb≡N–C≡C–N≡Nb core (Fig. 3, *left*). The HOMO and HOMO–1 reflect Nb–N and C–C multiple bonding, in accord with the structural metrics of **2**. The LUMO and LUMO + 1 are also part of this π-system, being Nb–N and C–C π-antibonding and N–C π-bonding in character.

The energetics of formation of **3** were calculated by DFT optimization of stationary points along a reaction coordinate describing the approach, interaction, and coupling of two equivalents of the model C-bound niobium(IV) cyanide complex (NC)Nb(N[Me]Ph)$_3$ (Fig. 3, *right*). Isomerization of (NC)Nb(N[Me]Ph)$_3$ (**A**) to the N-bound cyanide derivative (CN)Nb(N[Me]Ph)$_3$ (**C**) is thermodynamically uphill by 4 kcal mol^{-1} (ΔE_{elec} at 0 K)[35] and proceeds through the high-energy intermediate (η^2-CN)Nb(N[Me]Ph)$_3$ (**B**). Bringing two equivalents of (NC)Nb(N[Me]Ph)$_3$ together to form a singlet dimer linked by two μ,η^2:η^1-cyanide ligands (**D**) requires 19 kcal mol^{-1}. From this point forward, conversion to the C–C bonded *zig-zag* π-complex (μ,η^2:η^2-NCCN)-(Nb(N[Me]Ph)$_3$)$_2$ (**E**) and on to **3** (**F**) is a thermodynamically favored process, ending over 23 kcal mol^{-1} lower in energy than two spatially separated equivalents of (NC)Nb(N[Me]Ar)$_3$. This proposed mechanism is qualitatively similar to the one put forth by Cloke and co-workers to describe the reductive coupling of carbon monoxide to ethynediolate by [U(η^8-1,4-(Si-*i*-Pr$_3$)$_2$C$_8$H$_6$)(η^5-C$_5$Me$_5$)].[14] It is noteworthy that the related d^1 niobium cyanide complex (NC)Nb(N[*t*-Bu]Ar)$_3$ is stable and isolable and does not undergo reductive coupling.[36] This highlights the role that steric encumbrance plays in reaction pathways relevant to the formation of **2**, a subtlety not fully incorporated in DFT calculations employing a truncated ancillary ligand set.

Metal cyanogen complexes are typically prepared by substitution reactions where cyanogen displaces neutral ligands such as H$_2$O or CO.[37–39] The cooperative reduction and coupling of cyanide by two niobium(IV) centers, as described herein,
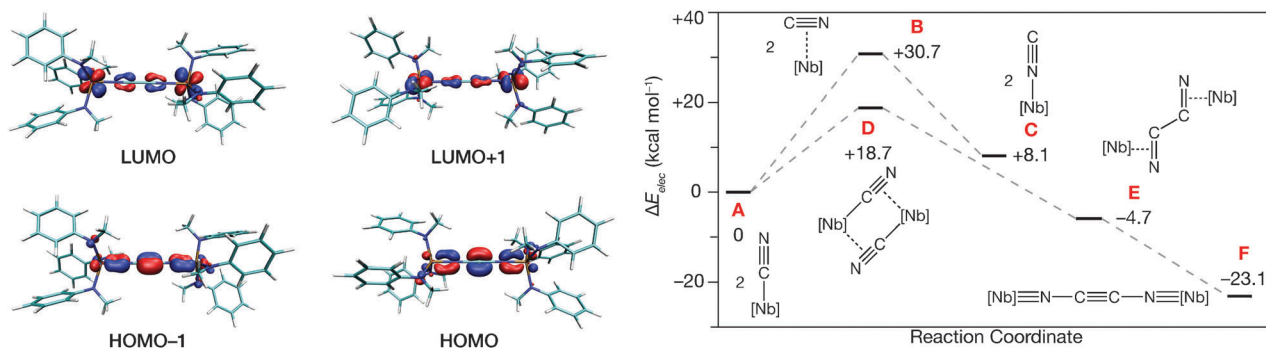
Fig. 3 *Left*: Frontier molecular orbitals of the model complex **3** illustrating the delocalized π-bonding across the heteropolyyne core. *Right*: Relative energies of stationary points describing the niobium-mediated reductive coupling of cyanide, where [Nb] = Nb(N[Me]Ph)$_3$.

demonstrates a new route to coordinated cyanogen derivatives and adds a new page to the long story of coupling reactions mediated by reducing metal complexes.

References

1 R. Fittig, *Liebigs Ann. Chem.*, 1859, **110**, 23.
2 B. E. Kahn and R. D. Rieke, *Chem. Rev.*, 1988, **88**, 733–745.
3 J. E. McMurry, *Chem. Rev.*, 1989, **89**, 1513–1524.
4 M. Ephritikhine, O. Maury, C. Villiers, M. Lance and M. Nierlich, *J. Chem. Soc., Dalton Trans.*, 1998, 3021–3028.
5 A. Gansauer and H. Bluhm, *Chem. Rev.*, 2000, **100**, 2771–2788.
6 E. J. Roskamp and S. F. Pedersen, *J. Am. Chem. Soc.*, 1987, **109**, 3152–3154.
7 W. J. Evans, C. A. Seibel and J. W. Ziller, *Inorg. Chem.*, 1998, **37**, 770–776.
8 H. A. Harris, A. D. Rae and L. F. Dahl, *J. Am. Chem. Soc.*, 1987, **109**, 4739–4741.
9 Y.-C. Tsai, F. H. Stephens, K. Meyer, A. Mendiratta, M. D. Gheorghiu and C. C. Cummins, *Organometallics*, 2003, **22**, 2902–2913.
10 E. M. Carnahan, J. D. Protasiewicz and S. J. Lippard, *Acc. Chem. Res.*, 1993, **26**, 90–97.
11 B. Wayland and X. F. Fu, *Science*, 2006, **311**, 790–791.
12 O. T. Summerscales, F. G. N. Cloke, P. B. Hitchcock, J. C. Green and N. Hazari, *Science*, 2006, **311**, 829–831.
13 O. T. Summerscales, F. G. N. Cloke, P. B. Hitchcock, J. C. Green and N. Hazari, *J. Am. Chem. Soc.*, 2006, **128**, 9602–9603.
14 A. S. Frey, F. G. N. Cloke, P. B. Hitchcock, I. J. Day, J. C. Green and G. Aitken, *J. Am. Chem. Soc.*, 2008, **130**, 13816–13817.
15 P. L. Arnold, Z. R. Turner, R. M. Bellabarba and R. P. Tooze, *Chem. Sci.*, 2011, **2**, 77–79.
16 M. P. Shores and J. R. Long, *J. Am. Chem. Soc.*, 2002, **124**, 3512–3513.
17 T. K. Brotherton and J. W. Lynn, *Chem. Rev.*, 1959, **59**, 841–883.
18 V. Chechik, M. Conte, T. Dransfield, M. North and M. Omedes-Pujol, *Chem. Commun.*, 2010, **46**, 3372–3374.
19 J. S. Figueroa and C. C. Cummins, *Dalton Trans.*, 2006, 2161–2168.
20 F. A. Cotton and W. T. Hall, *Inorg. Chem.*, 1978, **17**, 3525–3528.
21 F. A. Cotton and W. T. Hall, *J. Am. Chem. Soc.*, 1979, **101**, 5094–5095.
22 P. A. Finn, M. S. King, P. A. Kilty and R. E. McCarley, *J. Am. Chem. Soc.*, 1975, **97**, 220–221.
23 A. Mendiratta, C. C. Cummins, O. P. Kryatova, E. V. Rybak-Akimova, J. E. McDonough and C. D. Hoff, *Inorg. Chem.*, 2003, **42**, 8621–8623.
24 Modeling the bridging ligand as CNNC rather than NCCN leads to less favorable refinement statistics and produces a structural model that fails the Hirshfeld rigid-bond bond test (F. L. Hirshfeld, *Acta Crystallogr., Sect. A: Cryst. Phys., Diffr., Theor. Gen. Crystallogr.*, 1976, **32**, 239–244). Additionally, a disordered CNCN/NCNC model is inconsistent with the spectroscopic features of **2** and its isotopologues.
25 D. E. Wigley, *Prog. Inorg. Chem.*, 1994, **42**, 239–482.
26 F. H. Allen, O. Kennard, D. G. Watson, L. Brammer, A. G. Orpen and R. Taylor, *J. Chem. Soc., Perkin Trans. 2*, 1987, S1–S19.
27 H. W. Roesky, H. Hofmann, J. Schimkowiak, P. G. Jones, K. Meyer-Base and G. M. Sheldrick, *Angew. Chem., Int. Ed. Engl.*, 1985, **24**, 417–418.
28 T. M. Klapötke, H. Nöth, T. Schütt, M. Suter and M. Warchhold, *Z. Anorg. Allg. Chem.*, 2001, **627**, 1582–1588.
29 A. S. Parkes and R. E. Hughes, *Acta Crystallogr.*, 1963, **16**, 734–736.
30 A. L. Spek, *J. Appl. Crystallogr.*, 2003, **36**, 7–13.
31 W. Kemp, *Organic Spectroscopy*, Freeman, New York, 1991, p. 195.
32 The calculated normal modes of the DFT optimized model complex ($\mu,\eta^1:\eta^1$-NCCN)[Nb(NH$_2$)$_3$]$_2$ (ORCA *v.* 2.8: def2-TZV/BP86) include bands at 2220 cm^{-1} and 1162 cm^{-1} (uncorrected) that are primarily C–C and C–N stretching in character, respectively, but both modes display vibrational coupling across the Nb≡N–C≡C–N≡Nb core.
33 *Amsterdam Density Functional v2009.1*, 2009, http://www.scm.com.
34 I. Bytheway and M. W. Wong, *Chem. Phys. Lett.*, 1998, **282**, 219–226.
35 G. te Velde, F. M. Bickelhaupt, E. J. Baerends, C. F. Guerra, S. J. A. Van Gisbergen, J. G. Snijders and T. Ziegler, *J. Comput. Chem.*, 2001, **22**, 931–967.
36 M. G. Fickes, *PhD thesis*, Massachusetts Institute of Technology, 1998.
37 J. F. Guttenberger, *Angew. Chem., Int. Ed. Engl.*, 1967, **6**, 1081–1081.
38 G. Tom and H. Taube, *J. Am. Chem. Soc.*, 1975, **97**, 5310–5311.
39 S. Siddiqui, W. W. Henderson and R. E. Shepherd, *Inorg. Chem.*, 1987, **26**, 3101–3107.